Draft   January 30, 2004

The Ozone Mapping and Profiler Suite (OMPS)

Lawrence E. Flynn[1], Colin J. Seftor[2], Jack C. Larsen[2] and Philippe Xu[3]

[1]*NOAA/NESDIS*

5200 Auth Rd.

Camp Springs MD 20746

[2]Raytheon, Information Technology and Scientific Services

[3]IM Systems Group

X.1 Introduction

The Ozone Mapping and Profiler Suite (OMPS) is the next-generation US ozone monitoring system, designed for the National Polar-orbiting Operational Environmental Satellite System (NPOESS). The first flight of an OMPS is scheduled for late 2006 on the NPOESS Preparatory Project (NPP) satellite. The OMPS is designed to replace both the NASA Total Ozone Mapping Spectrometer (TOMS) and NOAA Solar Backscatter Ultraviolet Spectrometer/2 (SBUV/2) systems. The OMPS has two instrument modules: a combined Nadir Mapper and Nadir Profiler and a separate Limb Profiler.

The OMPS was designed to meet the stringent set of performance requirements for ozone products detailed in the original NPOESS system specifications. The instruments and algorithms were developed to give performance at least as good as the threshold requirements in Section 4.1.6.2.4 of the Integrated Operations Requirements Document (IORD). A copy of the IORD II is available at http://npoesslib.ipo.noaa.gov/Req_Doc/IORDII_011402.pdf. The specifications for the ozone Environmental Data Records (EDRs) from OMPS are given in Tables 1.a. and 1.b. A Dobson Unit (DU) is equivalent to a milli-atmosphere centimeter. This means, for example, that if all the ozone in an atmosphere with

a 300 DU column was collected at the surface at standard temperature and pressure, then it would form a gaseous layer 0.3 centimeters thick.

Table 1.a. Total Column Ozone EDR Performance

Measurement Parameter	Specification
Horizontal Cell Size	50 KM @nadir
Range	50 to 650 DU
Accuracy	15 DU
Precision	3 DU + 0.5%
Long-term Stability	1% over 7 years

Table 1.b. Ozone Profile EDR Performance

Measurement Parameter	Specification
Vertical Cell Size	3 km
Vertical Coverage	Tropopause to 60 KM
Horizontal Cell Size	250 KM
Range	0.1 to 15 ppmv
Accuracy	
Below 15 KM	Greater of 20% or 0.1 ppmv
Above 15 KM	Greater of 10% or 0.1 ppmv
Precision	
Below 15 KM	Greater of 10% or 0.1 ppmv
15 to 50 KM	Greater of 3% or 0.05 ppmv
50 to 60 KM	Greater of 10% or 0.1 ppmv
Long-term Stability	2% over 7 years

X.2 Nadir Sensors

Ozone has four main absorption bands in the ultraviolet, visible and near-infrared as follows: the Hartley bands from 200 – 310 nm, the Huggins bands from 310 – 380 nm, the Chappuis bands from 400 – 650 nm, and the Wulf bands from 600 – 1100 nm. The nadir sensor has two spectrometers, one with a wide, cross-track field-of-view (FOV) and spectral coverage in the Huggins ozone absorption bands, and the other with a smaller, nadir FOV and spectral coverage in the Hartley ozone absorption bands. Figures 1.a and 1.b show the ozone absorption cross-sections at a nominal atmospheric temperature for parts of these bands. (Figure 1.c. will be discussed later in the Limb Profiler Section.) Both sensors are designed to make measurements of the ratios of the ultraviolet radiance backscattered by the Earth's atmosphere/surface (BUV) to the extra-terrestrial solar irradiance. These ratios are called top-of-atmosphere albedos. The sensor detectors are 2-dimensional Charge-Coupled Devices (CCDs) arrays with spatial (cross-track) and spectral dimensions. The detectors are actively cooled to reduce dark current and radiation damage. Each of the nadir spectrometers samples the spectrum at 0.4 nm with 1-nm Full-Width-Half-Maximum (FWHM) end-to-end resolution. Long-term calibration stability is maintained by periodic solar observations using a Working and Reference reflective diffuser system similar to the system successfully deployed on the recent TOMS sensors.

The total column sensor has a 110° cross-track FOV and 0.27° along-track slit width. It has 35 cross-track bins. These are 3.35° (50 km) at nadir and 2.84° at ±55°. The resolution is 50 km along-track at nadir with a 7.6 second reporting period. The spectral coverage is from 300 to 400 nm, with the signal shared with the nadir profiler between 300 and 310 nm through the use of a dichroic beam splitter. The nadir profile sensor has a 16.6° cross-track FOV and 0.26° along-track slit width. Its 250x250 km cell size is collocated with the five central total column cells. The reporting period is 38 seconds synchronized with five reporting periods for the nadir mapper. The spectral coverage is from 250 to 310 nm.

X.3 Nadir Retrieval Algorithms

The nadir total column and vertical profile ozone retrieval algorithms build on the algorithms from the heritage systems, TOMS Version 7 (McPeters et al., 1996) and SBUV/2 Version 6 (Bartia et al., 1996). Information on the nadir and limb algorithms beyond that given is in the OMPS Algorithm Theoretical Basis Documents (ATBDs) at http://npoesslib.ipo.noaa.gov/atbd_omps.htm.

X.3.1 Total column ozone algorithm

Extensive studies and simulations using the TOMS Version 7 algorithm indicated that its performance was close to that needed to meet the NPOESS specifications for accuracy, and that it would provide a strong foundation for meeting NPOESS specifications for precision. The OMPS total column algorithm was therefore based on Version 7 of the TOMS algorithm with enhancements designed to improve its performance to meet the NPOESS requirements.

The algorithm uses triplets of wavelengths to obtain estimates of the total column ozone. Table values computed for a set of standard profiles, cloud heights, latitudes and solar zenith angles are interpolated and compared to the measured top-of-atmosphere albedos. The triplets combine an ozone insensitive wavelength channel (at 364, 367, 372 or 377 nm) to obtain cloud fraction and reflectivity information, with a pair of measurements at shorter wavelengths. The pairs are selected to have one "weak" and one "strong" ozone absorption channel. The hyperspectral capabilities of the sensor are used to select multiple sets of triplets to balance ozone sensitivity across the range of expected ozone column amounts and solar zenith angles. The "strong" ozone channels are placed at 308.5, 310.5, 312.0, 312.5, 314.0, 315.0, 316.0, 317.0, 318.0, 320.0, 322.5, 325.0, 328.0, or 331.0 nm. They are paired with a longer "weak" channel at 321.0, 329.0, 332.0, or 336.0 nm. Notice from Figure 1.a that the ozone cross-

sections decrease from 3 to 0.3 (atm.-cm)$^{-1}$ over the range of "strong" wavelengths. Typical ozone columns range from 100 DU or 0.1 atm-cm to 600 DU or 0.6 atm-cm. At the earth's surface, the attenuation of incoming solar flux due to an atmosphere with a total ozone column Ω is approximately given by $\exp[-s(\alpha\Omega + \beta p)]$ where s is the path length (approximately the secant of the solar zenith angle) and α is the ozone cross section. The quantity βp is the additional attenuation of the flux due to Rayleigh scattering. If the quantity $(s\alpha\Omega)$ is large, then the backscattered radiance is mainly composed of photons scattered from high in the atmosphere, and the corresponding channel has little information about the full ozone column. If the quantity $(s\alpha\Omega)$ is small, then the radiance has low sensitivity to any ozone changes. By varying the channels as viewing conditions and ozone amounts change, the algorithm is able to maintain good sensitivity to the full ozone column.

The hyperspectral capabilities of the sensor are further utilized through the selection of wavelengths with temperature-insensitive ozone cross-sections for use in the retrievals. Additional atmospheric temperature and ozone profile shape corrections are applied through the use of external temperature information obtained from NPOESS Cross-track Infrared Sounder (CrIS) measurements and external ozone profile information obtained from OMPS's own limb retrieval. The corrections are applied based on this external information through the use of first order expansions and retrieval sensitivity tables. If better tropospheric estimates than those in the standard ozone profile climatology are available, then a tropospheric ozone correction is applied to account for the inefficiency of the retrievals in sensing tropospheric ozone variations.

Simulations using synthetic radiances calculated from Stratospheric Aerosols and Gas Experiment (SAGE) ozone profiles and balloonsonde ozone and temperature profiles were used to demonstrate the improved performance from retrievals using the OMPS algorithm over retrievals using the TOMS V7

algorithm. These simulations have shown that the OMPS system performance is within the NPOESS specifications for total column ozone.

The retrieval algorithm includes calculations to identify atmospheres with high levels of aerosols. A quantity called the aerosol index is computed based on the differences between the measured versus modeled residuals for the 331- and 376-nm channels. This index is used to compute an adjustment to the ozone estimate to correct for wavelength-dependent effects of aerosols on the assumed reflectivity. See Torres et al. 1998 for more information.

The algorithm also identifies and flags atmospheres with large amounts of SO_2. The 310.5, 312.0, and 329.0 nm wavelength channels are chosen to compute an estimate of atmospheric SO_2. These wavelengths occur either at local maxima or minima with respect to the SO_2/O_3 cross-section ratios and were selected based on the conclusions in Gurevich and Krueger (1997) that such a choice optimizes the retrieval of SO_2. Since determination of the column SO_2 amounts requires knowledge of the height distribution, this estimate is just used as an index to identify regions with elevated levels of SO_2, which could result in errors in the ozone estimates.

X.3.2 Nadir profile ozone algorithm

The nadir profiler ozone algorithm is based on the heritage SBUV/2 maximum likelihood retrieval algorithm (Bhartia et al., 1996). The OMPS Nadir Profiler and Nadir Mapper make over 200 measurements across the spectral range covered by the twelve discrete measurements reported by the SBUV/2 instruments. The maximum likelihood algorithm can be adapted to use more measurements to provide a less noisy retrieval. The OMPS Nadir Profile sensor is designed with a double monochromator to give individual channel signal-to-noise ratio (SNR) performance at the SBUV/2 requirement levels, so the algorithm output even with just twelve wavelengths will be as good or better than the current operations. The

single-scattering, normalized weighting functions are shown in Figure 2. There are two sets of curves each for eight wavelengths from 252 nm to 306 nm. The curves show the penetration of photons into the atmosphere, and thus their sensitivity to ozone changes at different altitudes/pressures. The topmost dotted curve shows the results for 252 nm for 70º SZA. The bottommost dashed curve shows the results for 306 nm for 30º SZA. As the wavelengths increase, the ozone absorption cross-sections decrease (See Figure 1.b.) and the channels "see" deeper into the atmosphere. The weighting functions for the Nadir Profiler measurements produce broad contribution functions that cannot give adequate vertical resolution to meet the IORD ozone profile requirements. The Nadir Profiler will provide valuable data for the continuation of the SBUV/2 data record and validation and altitude registration for the Limb Profiler retrieval.

X.4 Limb Profiler (LP) Sensor

The limb sensor is based on the limb scattering technique developed for the Shuttle Ozone Limb Scattering Experiment/Limb Ozone Retrieval Experiment (SOLSE/LORE) (McPeters et al. 2000) and currently used for some of the measurements made by the Scanning Imaging Absorption Spectrometer for Atmospheric Chartography (SCIAMACHY), the Optical, Spectroscopic and Infrared Remote Imaging System (OSIRIS), and SAGE III. Plate 1 shows a view of the Earth's limb from the Space Shuttle. The OMPS Limb Profiler FOV will be similar to the LORE FOV with two additional FOVs spaced 250 km on either side.

The OMPS Limb Profiler prism spectrometers have spectral ranges from 290 to 1000 nm, with a resolution matched to the ozone absorption features. Polarization compensators minimize sensor polarization sensitivity. Cross-track samples are obtained with three separate slits/telescopes. Figure 3 shows sample model results. Notice the large dynamic range of signals over the range of tangent heights and wavelengths. The large scene dynamic range is covered by using two separate apertures in each telescope producing two optical gains

and by using two interleaved integration times producing two electronic gains. All six spectra (resulting from three slits viewed through two apertures) are captured on a single CCD focal plane. The window above the detector is coated with three different filters for the ultraviolet, visible and infrared regions of the spectra to reduce stray light. The limb sensor slits are separated by 4.25° (250 km at the tangent) and have a 38 second reporting period that equates to 250-km along-track motion. The Limb Profiler has a 2.23° vertical FOV equating to 130 km at the limb – 0 to 60 km atmospheric coverage plus offset allowances for pointing, orbital variation, and Earth oblateness.

X.5 Limb profiler ozone algorithm

The limb retrieval algorithm is based on the optimal estimation technique used in SOLSE/LORE retrievals and described in Flittner et al., 2000. The forward model uses the radiative transfer code developed at the University of Arizona by Ben Herman and Dave Flittner for NASA/GSFC. It generates a multiple scattering solution in a spherical atmosphere, including: molecular and aerosol scattering, ozone absorption, and polarization. The algorithm uses both ultraviolet and visible wavelengths to sense ozone variations. The algorithm uses height-normalized radiances and wavelength pairs and triplets to reduce the effects of reflectivity contributions to the limb scattered radiance and lessen the impact of instrument calibration and throughput changes. For example, the algorithm normalizes the visible channels by their radiances at 42 km, and then forms"visible triplets," ratios of the 600-nm channel radiances to the average of the 525-nm and 675-nm channel radiances. Notice in Figure 1.c. that the ozone absorption cross-section has a local maximum for the 600-nm channel.

Simulated results are given in Figures 4.a-c. The curves in Figure 4.a. show the 600-nm channel model radiances for a 40º SZA and mid-latitude 325 DU profile for three surface reflectivities cases (20, 50 and 80%) normalized to their values at 42 km. The radiances at 42 km for the 20 and 80% cases differ from the 50%

case by approximately –25% and +25%, respectively, prior to normalization. The curves in Figure 4.b. show the "visible triplet" results for the same model cases. Figure 4.c. shows how well the curves for the three reflectivity cases compare to each other. The values for the 20 and 80% reflectivity cases are divided by the values for the 50% reflectivity case. The thicker curves show the ratios for the triplet ratios for 20% and 80% to the triplet ratios for 50%. Notice that all three triplets stay within 3% of each other, meaning that an error in a modeled reflectivity should have little impact on the accuracy of a modeled triplet.

Plates 2.a and 2.b show the sensitivity of limb radiances at two selected channels and a range of tangent heights to ozone changes. Each curve shows how the radiance at a given observation tangent height would respond to relative changes in ozone in 1-km layers over a range of altitudes. The curves are given for tangent heights spaced every two kilometers. The exponential increase in pressure (scatterers) and the geometric increase in the path through the atmospheric layer at the tangent height, combine to give good vertical resolution, with the radiances often most sensitive to ozone changes in the layer at the tangent height. Because of the large attenuation along the Line-Of-Sight (LOS), due to both Rayleigh scattering and ozone absorption, the ultraviolet channels lose sensitivity as the tangent height moves down in the atmosphere. Rayleigh scattering increases inversely with the fourth power of the wavelength. The information for the ozone profile in the lower stratosphere is obtained from visible channels. The ozone absorption cross-sections for parts of the Chappuis and Wulf bands for the visible channels were shown in Figure 1.c.

The OMPS algorithm has been modified from the SOLSE/LORE basis to include additional ozone channels and a retrieval of the aerosol extinction profile by using wavelengths with little absorption by ozone. The Nadir Profiler ozone estimates are used as first guesses in the retrieval algorithm and to estimate the altitude registration of the limb profile measurements. The result is an algorithm that uses 25 **(XX CHECK XX)** spectral channels that will provide NPOESS ozone

profile EDR's with vertical coverage from the tropopause to 60 km. Plate 3 shows the channel locations and uses.

X.5.1 Limb retrieval complications

The Limb Profiler retrieval faces several complications. Three of the most serious are discussed here.

The first major source of error discussed here for the limb retrievals is altitude registration of the measurements. The long distance from the satellite to the limb poses a critical problem for pointing accuracy and precision. Small uncertainties and variations in the spacecraft attitude or alignment are magnified by the 3300 km LOS from the spacecraft to the atmospheric limb tangent point. A 10-arc second error in pitch becomes a160-meter error at the limb tangent. The algorithm attempts to estimate the height registration by matching limb radiances calculated by using ozone profile information from the nadir sensor with radiances measured by the limb sensor. Simulations indicate that, even with this correction, there is a 300-meter uncertainty in the altitude registration, and ozone retrieval precision errors from 15 to 28 km are still above the NPOESS requirements. This is primarily due to the errors in regions with large vertical ozone gradients. If the orbital variations are repeatable, it should be possible to reduce the height registration errors even farther through statistical analysis.

A second source of error occurs due to effects of variations in reflectivity. Unlike occultation measurements where almost all of the photons for an observation at a given tangent height follow the same path through the atmosphere along the entire LOS, the photons in a limb scatter measurement are scattered toward the instrument from different locations along the LOS. The height normalization computations assume that the measurements at different tangent heights are the result of interactions with similar surface and cloud reflectivity. There are two main problems with this assumption. If we compare the photons scattered into a

LOS from below for a 60-km tangent height with those for a 20-km tangent height above the same Earth location, then we find that the 60-km LOS sees a wider across-track area. If there are variations in the surface and cloud reflectivities across-track, then these will affect the two measurements differently.

Further, since the optical depth to a point along the LOS increases with decreasing tangent height, the two measurements will also be affected differently by reflectivity variations below the LOS nearer and farther from the satellite. As the tangent height decreases a larger portion of the photons come from light scattered in the nearer part of the LOS. Cases with large variations will occur when a LOS extends from over the open ocean to over an ice field. If, for example, the reflectivity below the LOS has a transition from 80% to 20% near the sub-tangent point, then the effective reflectivity will vary as the tangent height changes. If the reflectivity nearer to the satellite is 80% (or 20%) then the radiance will become more like the 80% (or 20%) homogeneous case as the tangent height decreases. The increase in optical depth to a point along the LOS as the tangent height dereases is not the same for different wavelength channels as it depends on absorption and scattering properties. Thus the real measurments from the atmosphere will not behave as nicely as represented in Figure 4.c. The normalized radiances for sharp contrast and other varying refelctivity case can deviate from the homogeneous case and without additional modeling could be interpreted as erroneous ozone or aerosol profile variations. Forward models with varying underlying reflectivity are under development to address this problem.

A third source of error is related to the simplified representation of the 3-D ozone field. The photons scattered toward the satellite within the line of sight travel different distances through the atmosphere along the LOS. This means that they are differentially sensitive to ozone variations along the LOS. The basic retrieval algorithm assumes that the ozone field has local spherical symmetry, that is, that the ozone in a given vertical layer is the same for the paths for the different

tangent heights. In reality, for example, the LOS for a 30-km tangent height passes through the 1-km layer between 40 and 41 km over 350 km away from the tangent point (once on the near side and again on the far side). The assumption of spherical symmetry may not give accurate results. The limb scattering arrangement does not even have the balancing of linear ozone gradients present for occultation observations. For occultations, if there is a linear ozone gradient in a layer, then the same photons will pass through both the elevated and lowered concentration regions relative to the layer amount at the tangent. For limb scattering, more photons will pass through the nearer layer than the farther one, adding to the discrepancy between a spherically symmetric model and reality. Multi-pass retrievals and tomographic approaches using 3-D ozone fields have been developed and tested and offer some promise for reducing the errors from this complication.

Measurements from the Limb Profiler on OMPS on NPP will be used to develop and test solutions to these and other complications. For more information on the current status of the OMPS and NPOESS, please visit the NPOESS web site at http://www.ipo.noaa.gov.

X.6 REFERENCES

Bhartia, P.K., R.D. McPeters, C.L. Mateer, L.E. Flynn, and C. Wellemeyer, "Algorithm for the estimation of vertical ozone profiles from the backscattered ultraviolet technique," *J. Geophys. Res.*, **101**, 18793-18806, 1996.

Flittner, D.E., B. Herman, and P.K. Bhartia, "The retrieval of ozone profiles from limb scatter measurements: Theory," *Geophys. Res. Lett.*, **27**, 2601-2604, 2000.

Gurevich, G.S. and A.J. Krueger, "Optimization of TOMS wavelength channels for ozone and sulfur dioxide retrievals," *Geophys. Res. Lett.*, **24**, 2187-2190, 1997.

McPeters, R.D., et al. Nimbus-7 TOMS Data Products User's Guide, NASA Reference Publication #1384, 1996.

McPeters, R.D., S. Janz, E. Hilsenrath, T. Brown, D. Flittner, and D. Heath, "The retrieval of ozone profiles from limb scatter measurements: Results

from the Shuttle Ozone Limb Sounding Experiment," *Geophys. Res. Lett.*, **27**, 2597-2600, 2000.

Torres, O., P.K. Bhartia, J.R. Herman, Z. Ahmad, and J. Gleason, "Derivation of aerosol properties from satellite measurements of backscattered ultraviolet radiation: Theoretical basis," *J. Geophys. Res.,* **103**, 17099-17110, 1998.

The IORD II is available from a link at
http://www.ipo.noaa.gov/Library/techreq_NDX.html
It is at http://npoesslib.ipo.noaa.gov/Req_Doc/IORDII_011402.pdf
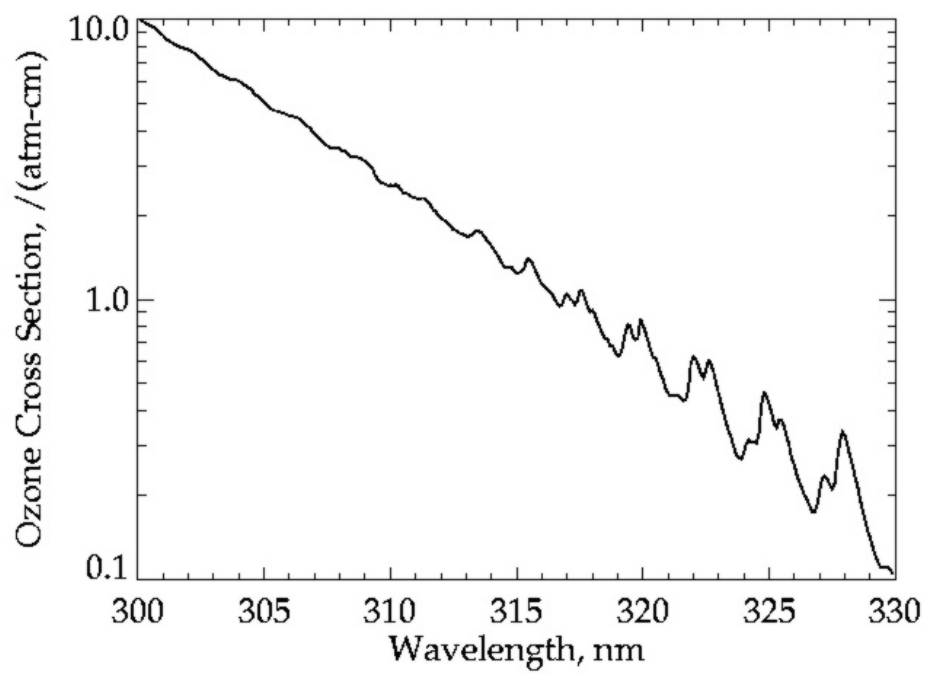
Figure and Plate Captions

Figure 1.a. Ozone absorption cross-sections in the Huggins bands.
Figure 1.b. Ozone absorption cross-sections in the Hartley bands.
Figure 1.c. Ozone absorption cross-sections in the Chappuis and Wulf bands.

Figure 2. Weighting functions for the eight shortest SBUV/2 profile wavelengths – 252, 273, 283, 288, 292, 298, 302, and 306 nm – for a standard 325 mid-latitude profile at two SZAs. The curves show the relative sensitivity of each channel to ozone changes as a function of height. Each curve is normalized by its peak sensitivity. The ozone absorption cross-section decreases with increasing wavelength so more photons penetrate deeper into the atmosphere.

Figure 3. Simulated radiances for selected channels for limb scattering observations. The curves give the radiances for different wavelength channels as functions of tangent height in km. The model atmosphere used a standard mid-latitude 325 DU total column ozone profile and a 40º SZA.

Figure 4.a. Normalized radiances as a function of tangent height. The curves show the 600-nm model radiances for a 40º SZA and mid-latitude 325 DU profile for three surface reflectivities cases (20, 50 and 80%) normalized to their values at 42 km. The radiances at 42 km for the 20 and 80% cases differ from the 50% case by approximately –25% and +25%, respectively, prior to normalization.
Figure 4.b. Visible triplet radiance ratios as a function of tangent height. The curves show the ratios of the 600-nm model radiances for a 40º SZA and mid-latitude 325 DU profile for three surface reflectivity cases (20, 50 and 80%) to the averages of the similarly computed 675 and 525-nm channels radiances. All the results are further normalized to their values at 42 km.
Figure 4.c Deviations in normalized radiances for reflectivity cases. The curves show the ratios of the 600-nm model radiances for a 40º SZA and mid-latitude 325 DU profile for 20% and 80% surface reflectivity compared to the model results for a 50% reflectivity case versus tangent height in km. The thicker curves show the ratios for the triplet ratios for 20% and 80% to the triplet for 50%. The triplet ratios are the ratios of the 600-nm channel radiances to the averages of the 675 and 525-nm channels radiances. All the results are further normalized to their values at 42 km.

Plate 1. View of the Earth's limb from the Space Shuttle. The OMPS Limb profiler will fly in a higher orbit so its 2.23º vertical FOV will give altitude coverage similar to LORE's.

Plate 2.a. Sensitivity of the 305-nm channel limb radiances to layer ozone changes for 1-km layers. Each curve gives the ratio of changes in the limb radiance for a given tangent height to changes in the ozone amounts as a function of altitude. The changes in the natural log of both quantities are used to give a %radiance change / %ozone change interpretation to the results. The curves give radiances for tangent heights spaced out every 2 km.

Plate 2.b. Same as Plate 2.b except for the 600-nm channel.

Plate 3. Channel positions and uses for the Limb Profiler retrieval algorithm.

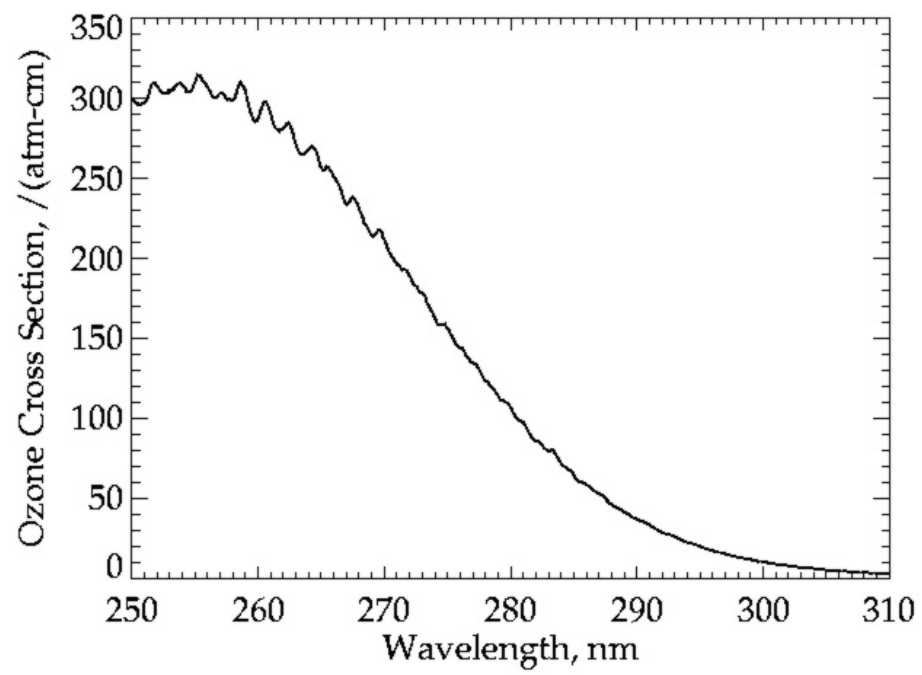Figure 1.a. Ozone absorption cross-sections in the Huggins bands.

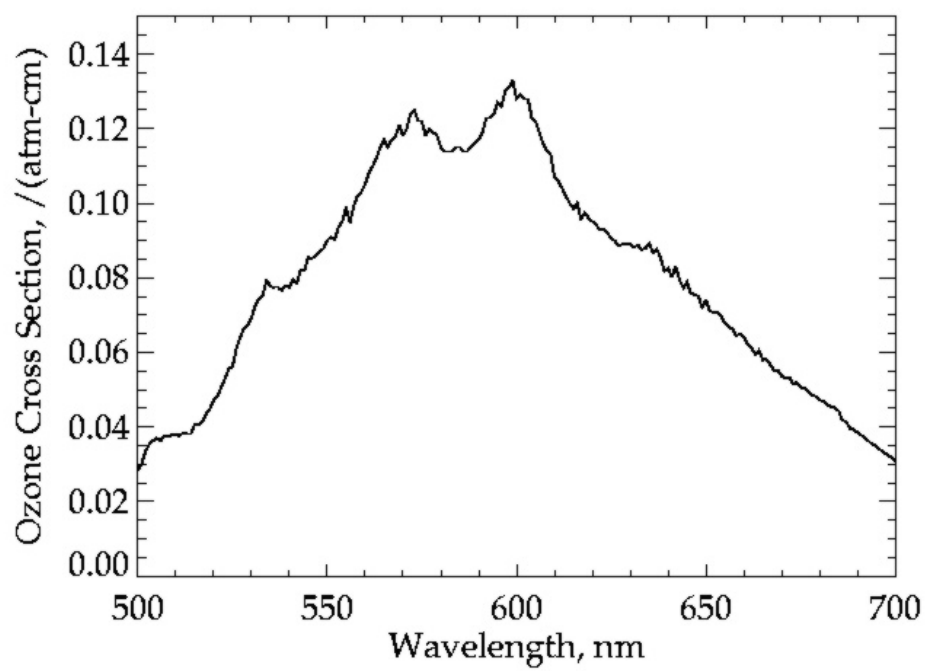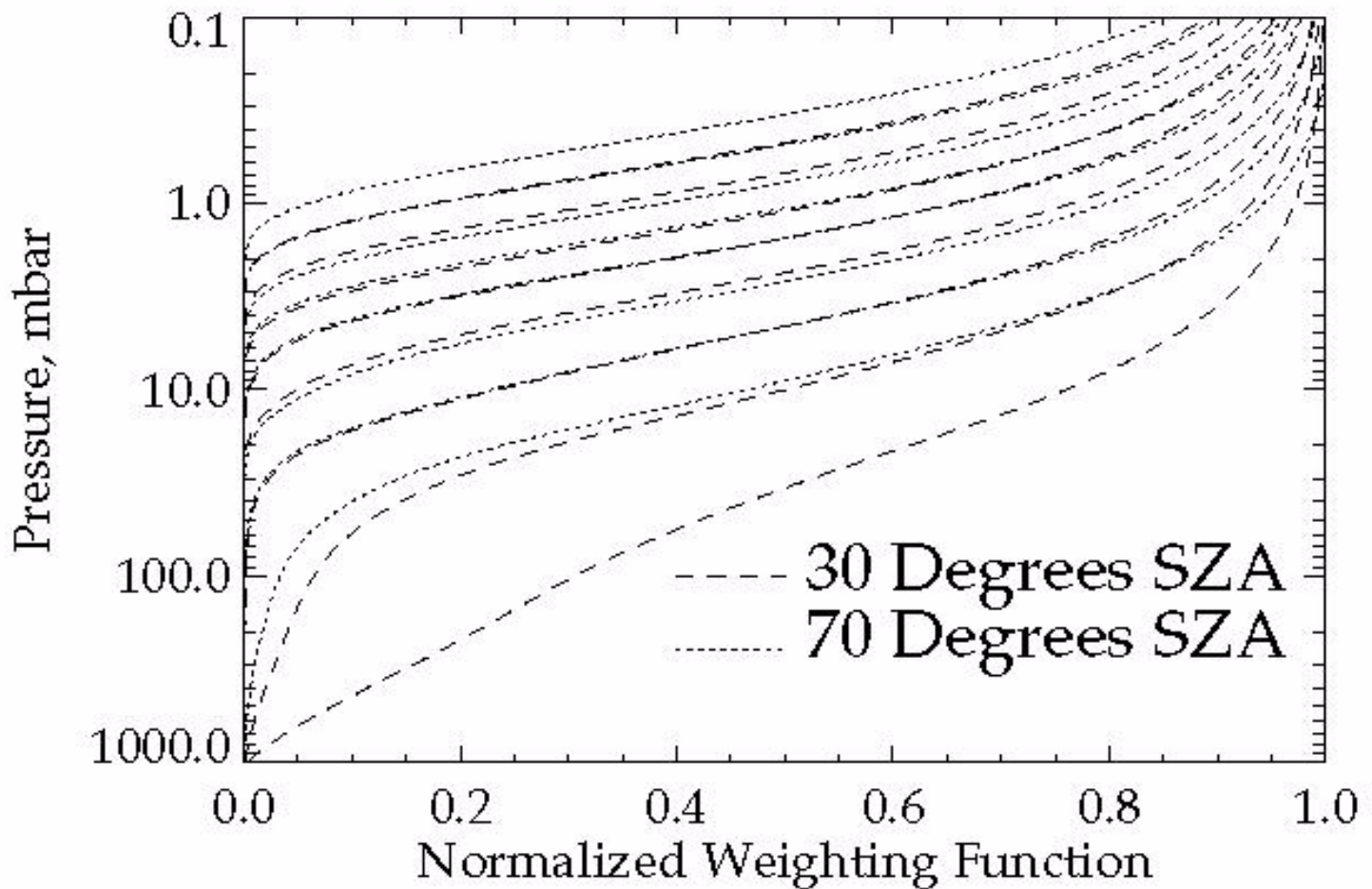Figure 1.b. Ozone absorption cross-sections in the Hartley bands.

Figure 1.c. Ozone absorption cross-sections in the Chappuis and Wulf bands.

Figure 2. Weighting functions for the eight shortest SBUV/2 profile wavelengths – 252, 273, 283, 288, 292, 298, 302, and 306 nm – for a standard 325 mid-latitude profile at two SZAs. The curves show the relative sensitivity of each channel to ozone changes as a function of height. Each curve is normalized by its peak sensitivity. The ozone absorption cross-section decreases with increasing wavelength so more photons penetrate deeper into the atmosphere.
XX Label Some Curves XX
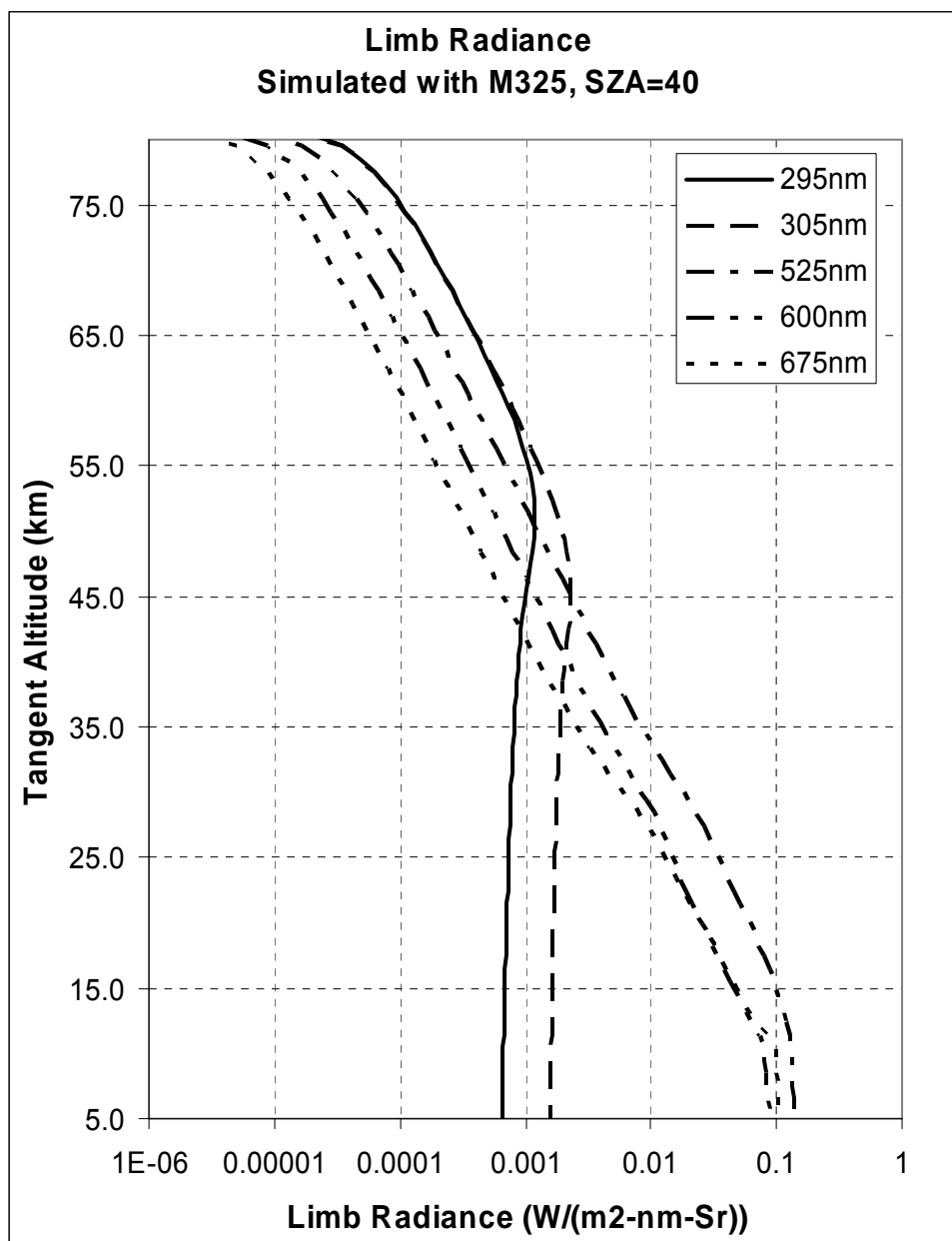
Figure 3. Simulated radiances for selected channels for limb scattering observations. The curves give the radiances for different wavelength channels as functions of tangent height in km. The model atmosphere used a standard mid-latitude 325 DU total column ozone profile and a 40º SZA.

Figure 4.a. Normalized radiances as a function of tangent height. The curves show the 600-nm model radiances for a 40º SZA and mid-latitude 325 DU profile for three surface reflectivities cases (20, 50 and 80%) normalized to their values at 42 km. The radiances at 42 km for the 20 and 80% cases differ from the 50% case by approximately –25% and +25%, respectively, prior to normalization.

Normalized Triplet Radiance
Band 600/525,675, M325, SZA=40
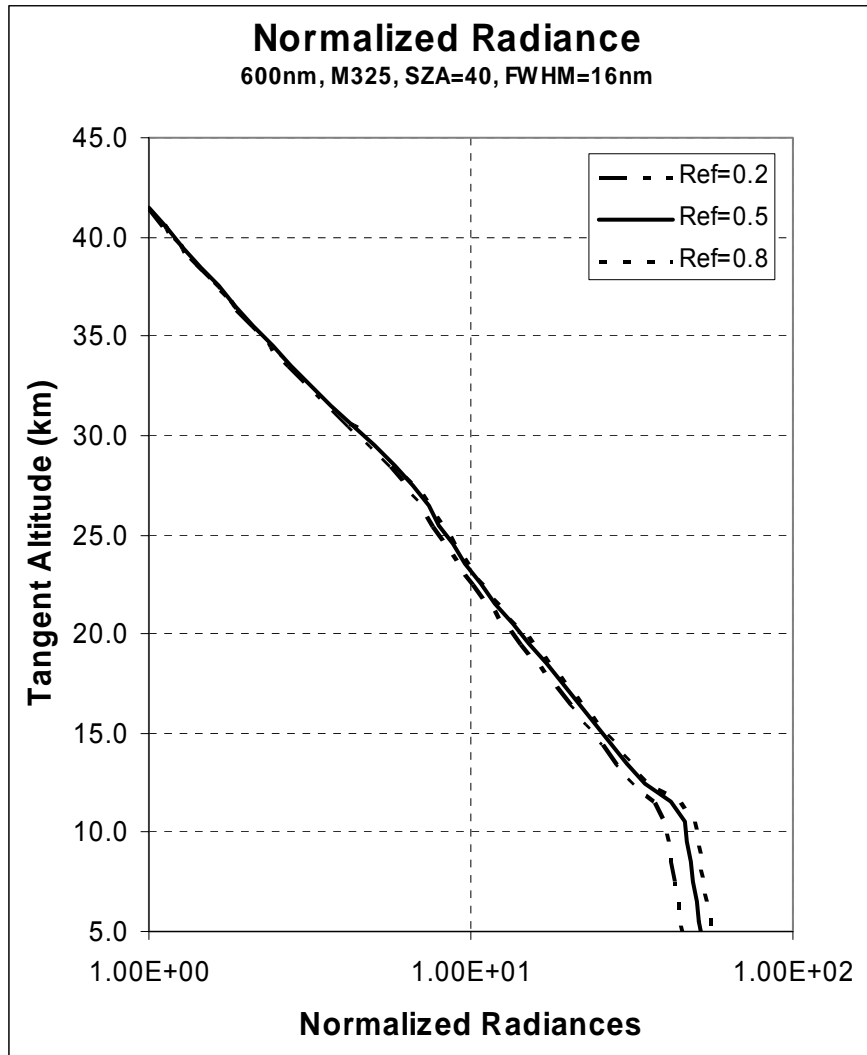
Figure 4.b. Visible triplet radiance ratios as a function of tangent height. The curves show the ratios of the 600-nm model radiances for a 40° SZA and mid-latitude 325 DU profile for three surface reflectivity cases (20, 50 and 80%) to the averages of the similarly computed 675 and 525-nm channels radiances. All the results are further normalized to their values at 42 km.
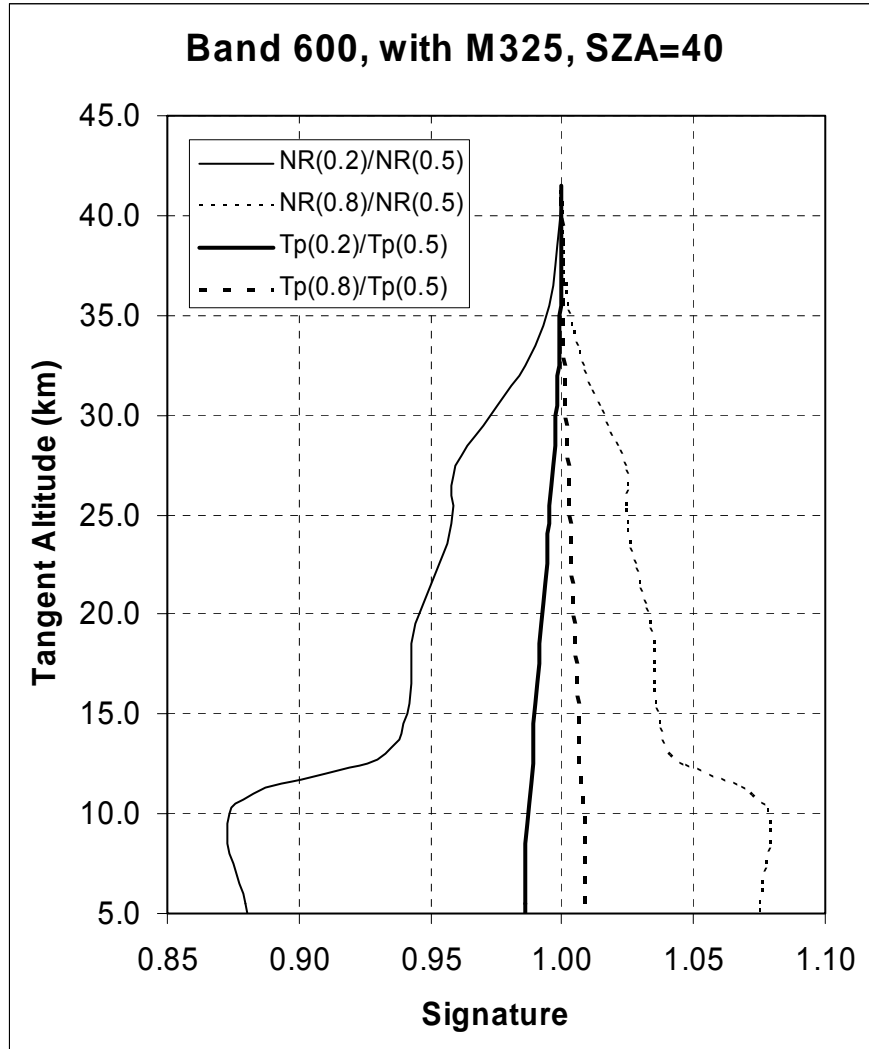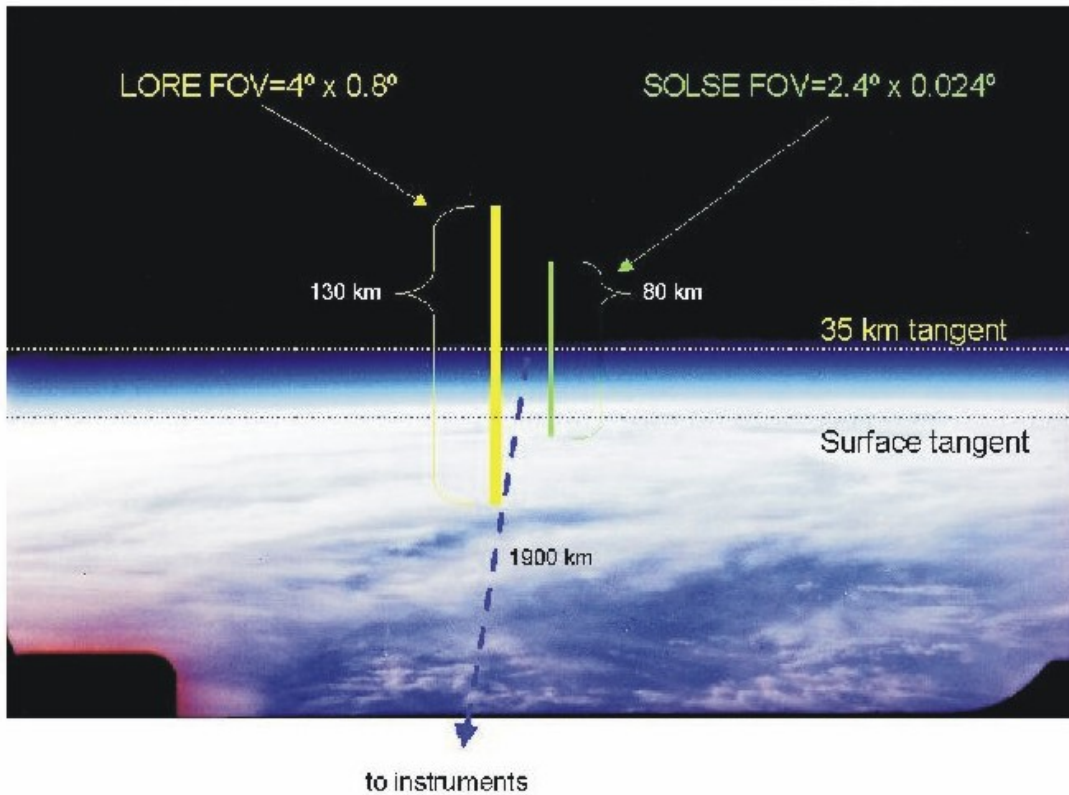
Figure 4.c Deviations in normalized radiances for reflectivity cases. The curves show the ratios of the 600-nm model radiances for a 40º SZA and mid-latitude 325 DU profile for 20% and 80% surface reflectivity compared to the model results for a 50% reflectivity case versus tangent height in km. The thicker curves show the ratios for the triplet ratios for 20% and 80% to the triplet for 50%. The triplet ratios are the ratios of the 600-nm channel radiances to the averages of the 675 and 525-nm channels radiances. All the results are further normalized to their values at 42 km.

Plate 1. View of the Earth's limb from the Space Shuttle. The OMPS Limb profiler will fly in a higher orbit so its 2.23º vertical FOV will give altitude coverage similar to LORE's.

Plate 1. is a taken from

http://code916.gsfc.nasa.gov/Public/Space_based/solse/results.html
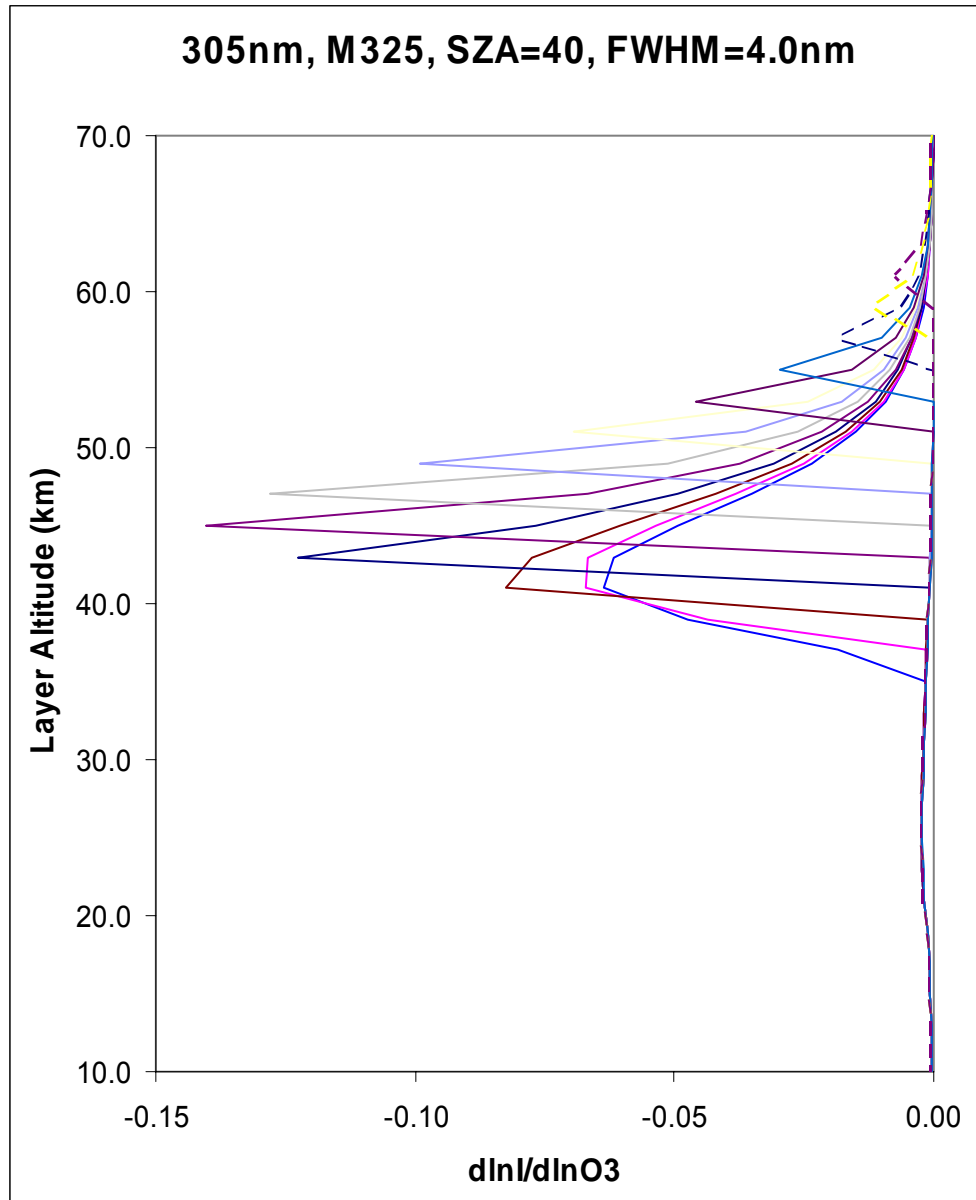
XXSharper BracketsXX

Plate 2.a. Sensitivity of the 305-nm channel limb radiances to layer ozone changes for 1-km layers. Each curve gives the ratio of changes in the limb radiance for a given tangent height to changes in the ozone amounts as a function of altitude. The changes in the natural log of both quantities are used to give a %radiance change / %ozone change interpretation to the results. The curves give radiances for tangent heights spaced out every 2 km.
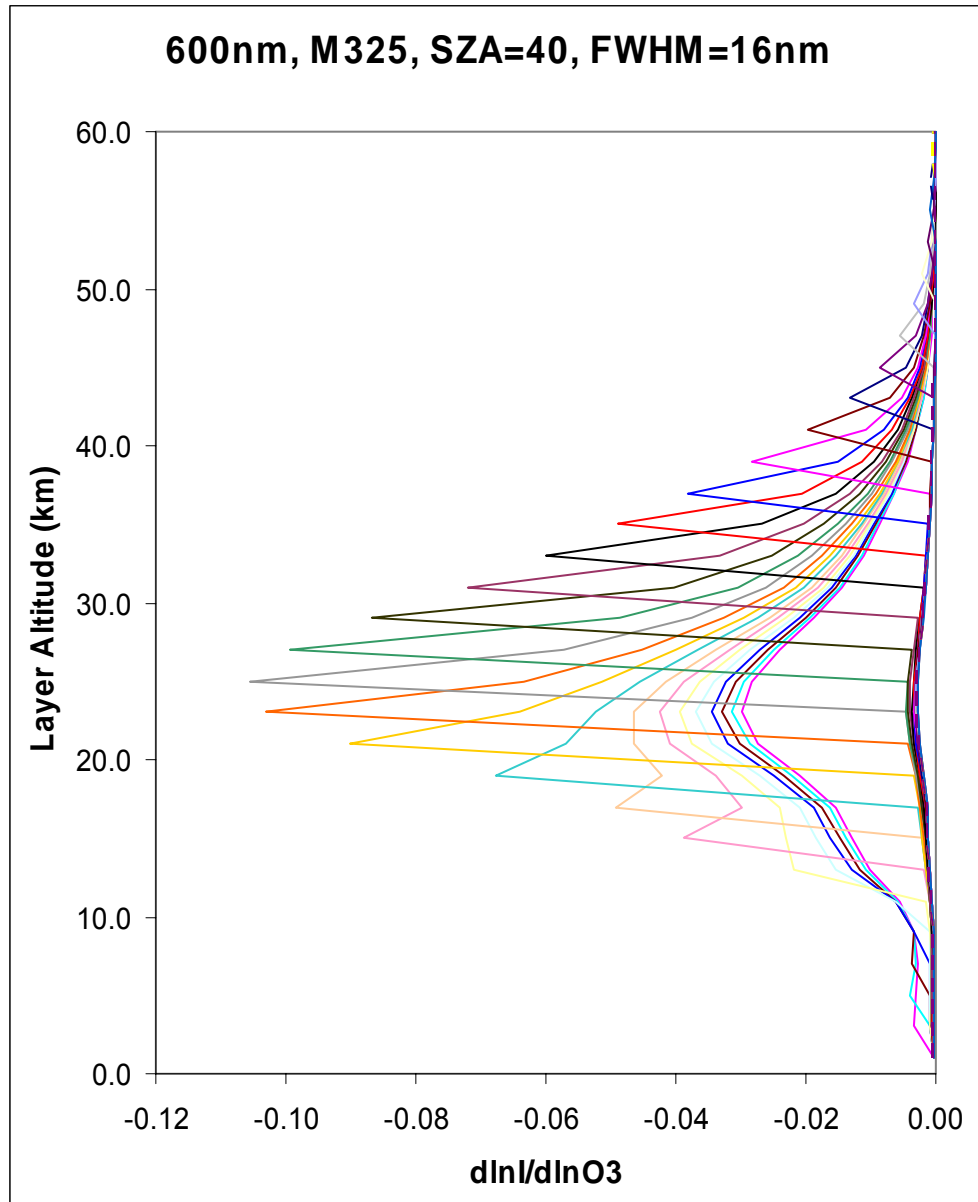
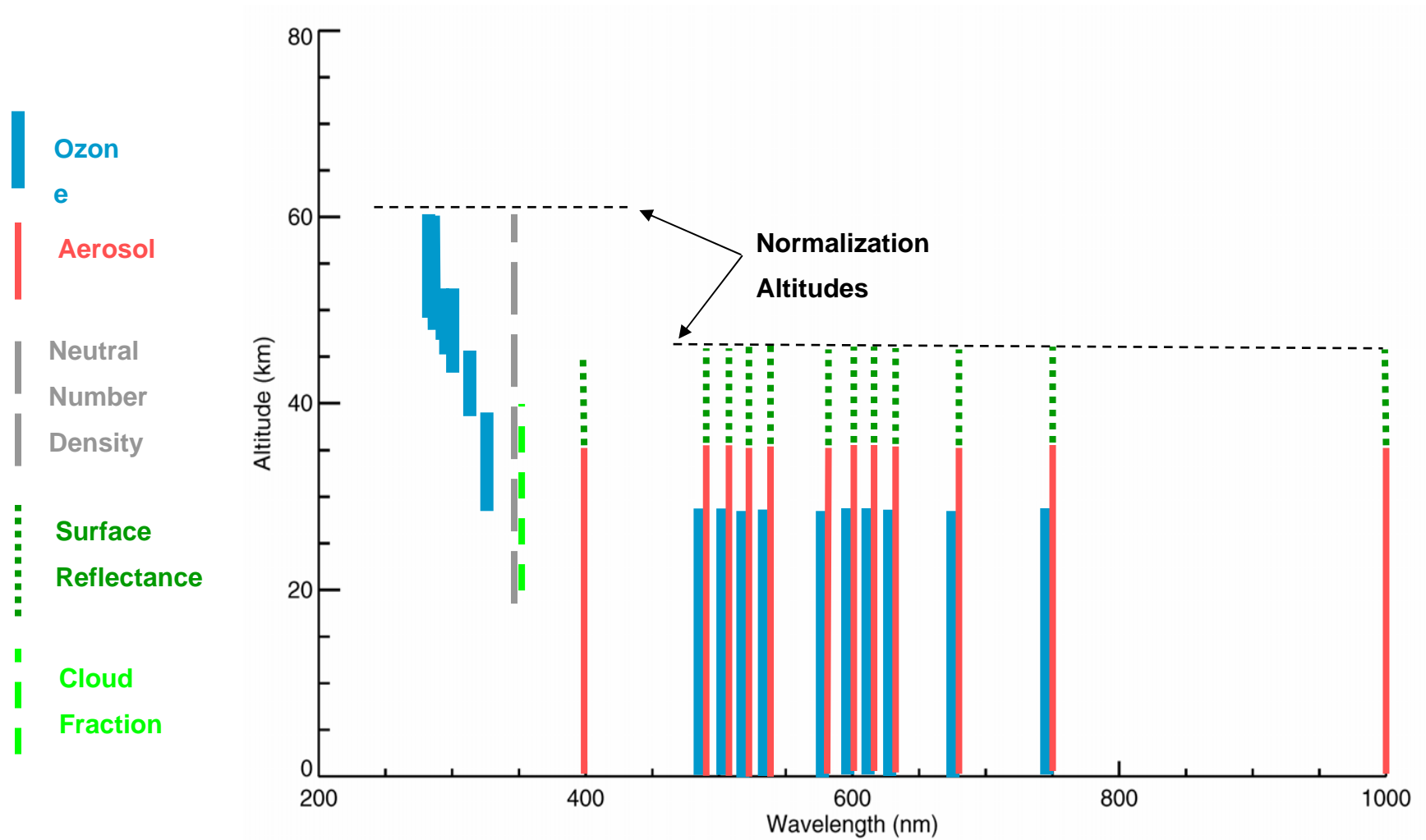Plate 2.b. Same as Plate 2.b except for the 600-nm channel.

Plate 3. Channel positions and uses for the Limb Profiler retrieval algorithm.

XXCheck Current ChannelsXX